

Diminishing Return for Increased Mappability with Longer Sequencing Reads: Implications of the k -mer Distributions in the Human Genome

Wentian Li^{1,*}, Jan Freudenberg¹, Pedro Miramontes²

1. *The Robert S. Boas Center for Genomics and Human Genetics*

The Feinstein Institute for Medical Research

North Shore LIJ Health System

Manhasset, 350 Community Drive, NY 11030, USA.

2. *Departamento de Matemáticas, Facultad de Ciencias*

Universidad Nacional Autónoma de México, Circuito Exterior

Ciudad Universitaria, México 04510 DF, México.

*To whom correspondence should be addressed. Email: wtli2012@gmail.com

Abstract

The amount of non-unique sequence (non-singletons) in a genome directly affects the difficulty of read alignment to a reference assembly for high throughput-sequencing data. Although a greater length increases the chance for reads being uniquely mapped to the reference genome, a quantitative analysis of the influence of read lengths on mappability has been lacking. To address this question, we evaluate the k -mer distribution of the human reference genome. The k -mer frequency is determined for k ranging from 20 to 1000 basepairs. We use the proportion of non-singleton k -mers to evaluate the mappability of reads for a corresponding read length. We observe that the proportion of non-singletons decreases slowly with increasing k , and can be fitted by piecewise power-law functions with different exponents at different k ranges. A faster decay at smaller values for k indicates more limited gains for read lengths > 200 basepairs. The frequency distributions of k -mers exhibit long tails in a power-law-like trend, and rank frequency plots exhibit a concave Zipf's curve. The location of the most frequent 1000-mers comprises 172 kilobase-ranged regions, including four large stretches on chromosomes 1 and X, containing genes with biomedical implications. Even the read length 1000 would be insufficient to reliably sequence these specific regions.

Introduction

Many applications of next-generation-sequencing (NGS) in human genetic and medical studies depend on the ability to uniquely align DNA reads to the human reference genome (1–6). This in turn is related to the level of redundancy caused by repetitive sequences in the human genome, well known in the earlier human whole-genome shotgun sequencing (7–9), and the read length k . When the read length is too short, it is theoretically impossible to construct a sequence with size comparable to the human genome that does not contain any repeats of windows with k bases. It has been shown using graph theory that the shortest DNA sequences avoiding any repeats of k -mers can be constructed by packing all unique k -mers shifting one position at the time (10). The number of different k -mer types is $4^k/2$ (k even) or $(4^k + 2^k)/2$ (k odd) if both a subsequence and its reverse complement are considered to belong to the same k -mer type. Solving $4^k/2 \approx 3 \times 10^9$ leads to the conclusion that read length k must be at least greater than 17 for all reads to be uniquely alignable to a hypothetical reference sequence that has the size of the human genome.

However, in reality the human genome did not evolve by a first principle to be consistently compact and incompressible. Redundant sequences in the human genome have resulted from duplication, insertion of transposable elements, and tandem repeats due to replication slippage, and more than half of the human genome can be traced to repetitive transposable elements. Although locally duplicated sequences can be deleterious (11) or disease-causing (12), a certain level of redundancy is crucial for biological novelty and adaptation (13–15). For higher eukaryotes, a slower removal of the deleterious repeats due to low mutation rates and smaller population sizes (16) lead to a higher level of genome-wide redundancy. This in turns may lead to more protein sequences with internal repeats and perhaps new fold or new functions such as the case for connection tissue, cytoskeletal, and muscle proteins (17).

Therefore, $k=17$ is a very unrealistic estimation of the minimal read length required for a perfectly successful NGS reads alignment. Accordingly, NGS technologies utilize reads with various larger lengths: $k=70$ for *Complete Genomics*, $35 \sim 85$ for *ABI SOLiD*, $75 \sim 150$ pair-end for *Illumina HiSeq*, 400 for *Ion Torrent PGM*, $450 \sim 600$ for *Roche 454 GS FLX Titanium XLR70*, etc. (18). Currently, the technology is pushing towards read lengths of $k=1000$ (e.g.,

Roche 454 GS FLX Titanium XL+) or even $k=10000$ (19). Needless to say, the longer the read length, the higher the chance that reads can be aligned to the reference genome. Ultimately, high quality genome will be obtained by a mix of technologies. To find this optimal mixture, a quantitative understanding of the repeat structure of the human genome is required.

Our analysis of the repeat structure is different from some earlier investigations of read mappability (3, 5). In these studies, the actual reads from the current sequencing technology are used. There are two shortcomings in these approaches: (i) it is impossible to extrapolate the result to read lengths which is beyond the current technology; (ii) a certain proportion of reads are never mappable because the corresponding regions in the reference genome are not finished. Using the existing reference genome makes it possible to treat k -mers as hypothetical reads whose length k can be as long as possible, and unfinished regions can be excluded from the analysis.

In this paper we quantitatively address the question of how alignment improves for greater read lengths. To this end we artificially cut the human reference genome into overlapping k -windows (k -mers, k -tuples, or k -gram (20)), each considered to be possible a “read”, and count the number of appearances (or “tokens”, borrowing a terminology from linguistics (21)) of each k -mer type across the full reference sequence. Those k -mer types that appear in the genome only once ($f=1$) are labeled singletons, and the remainder ($f > 1$) are non-singletons. Intuitively, the percentage of non-singleton reads is expected to decrease with increasing read length k . Obtaining the functional form of this decay enables us to predict the percentage of difficult-to-align reads at longer k 's.

These seemingly simple calculations already encounter a “big data” problem on a regular-sized computer. In particular, storing counts in a hash table requires large amount of RAM. Suppose a k -mer needs K byte to store (e.g. $K=k/4$), a hash table to count all k -mers in the human genome would require $3K$ GByte RAM, which quickly becomes implausible when k is greater than 100. Using a solution that is similar to other applications where the hard disk (22–24) or computing time (25) is traded with RAM, we use a new public-domain program DSK which utilizes the less expensive hard disk or longer CPU time to compensate a lack of RAM (26). Other efficient k -mer count procedures have been proposed in (27–29).

The mathematical relationship between the fraction of non-singleton k -mers and k predicts

the fraction of putative reads that can be mapped uniquely. Another statistic of interest is the distribution of k -mer frequencies when k is fixed at a given value. This distribution has a head and a tail, a head for low frequency k -mers (including singletons), and a tail for high frequency k -mers. In the situation when these distributions exhibit long-tails (30) and power-law-like trends (31), thus fitting a straight line in log-log scale, the head end is best characterized by the frequency distribution (21), whereas the tail end is better characterized by the rank-frequency distribution commonly related to Zipf's law in quantitative linguistics (32). Our analysis of these distributions provides information on the level of redundancy in the human genome at various scales.

Locating human genome regions that cannot be uniquely mapped by sequencing reads (which can be called "non-uniqueome" following the term "uniqueome" used in (3)) is important in any NGS-based studies. These regions may contribute the most to the false-positive and false-negative variant callings. These may also be hotspot for other structural variations such as indel and copy-number-variation (33, 34). We will specifically examine the location of some of these redundant regions at the $k = 1000$ level.

MATERIALS AND METHODS

Genome sequence data

The human reference genome GRCh37 (hg19) was downloaded from UCSC's genome browser (<http://genome.ucsc.edu/>). The intermittent strings of N's (marking unfinished basepairs that cannot be sequenced with the applied technology (35)) are used to partition the 22 autosomes and 2 sex chromosomes into 322 subsequences, and k -mers overlapping two chromosome partitions are not allowed.

For an additional analysis on repeat-filtered sequences, strings of lowercase letters in the reference genome (which mark repetitive sequences identified by the RepeatMasker program, <http://www.repeatmasker.org/>) are used to partition the genome into 3456905 subsequences with all transposable elements removed.

Counting k -mers

A k -mer type includes both the direct and the reverse complement substring; AAGC/GCTT is an example of such a 4-mer type. We use a state-of-art k -mer counting program DSK (26) (<http://minia.genouest.org/dsk/>), version 1.5031 (March 26, 2013). Most of the DSK calculations were carried out on a Linux computer with 48 GByte RAM and around 900 GByte disk space, except a calculation at $k=1000$ which was run on another Linux computer with the same RAM but 30 TByte of disk space. The parameter setting of DSK was determined by a trial-and-error process. The output of the DSK program consists of a list of k -mers. The BLAT program from UCSC's genome browser is used to map frequent k -mers back to the reference genome.

Frequency distribution, rank frequency plot, and data fitting

Suppose a k -mer type appears in the genome f times (f is frequency, or copy number); frequency distribution (FD) is the number of k -mer types with frequency f . Individual k -mer types can be ranked by their f , highest f ranks number 1, second highest f ranks number 2, etc. The ranked f 's of k -mer types as a function of rank r is the rank-frequency distribution (RFD).

The functions used here in fitting the RFD can all be expressed as linear regression, include Weibull function: $\log(f) \sim \log(\log((\max(r) + 1)/r))$ (36); quadratic logarithmic: $\log(f) \sim \log(r) + (\log r)^2$ (37); and reverse Beta: $\log(r) \sim \log(f) + \log(\max(f) + 1 - f)$. The latter function is derived from the Beta rank function (38, 39) by reversing the f and r . All linear regressions are carried out by the *R* function *lm* (<http://www.r-project.org/>).

RESULTS

Percentage of non-singleton reads vs. read length: piece-wise power-law function

In Figure 1 we show the percentage of non-singleton reads/tokens (p_{ns}) as a function of k -mer length k in log-log scale. The p_{ns} is 28.35% at $k=20$, 8.16% at $k=50$, 4.26% at $k=80$, 3.40% at $k=100$, 2.44% at $k=150$, 1.33% at $k=400$, 1.18% at $k=500$, and 0.82% at $k=1000$. If k is

shorter than the “shortest unique substring” length, which is 11 in the human genome (40), singletons do not exist (i.e., $p_{ns} = 100\%$).

Visual inspection of the trend suggests the use of piecewise power-law function in fitting the data. We fit the points in $k = 20-80$ and $k = 200-1000$ ranges separately by linear regressions in the log-log scale: $\log_{10} p_{ns} = a + b \log_{10} k$ (or $\log p_{ns} \sim \log k$). The fitted (\hat{a}, \hat{b}) is $(1.58366, -1.5478)$ and $(-0.4371, -0.5495)$ for the two segments, equivalent to $p_{ns} = 38.34/k^{1.548}$ and $p_{ns} = 0.365/k^{0.55}$. The steep decay in the first segment shows a stronger increase of the amount of uniquely mappable sequences with read length, which implies that obtaining read lengths of at least around 100 is more cost-efficient with respect to reducing the amount of non-mappable reads. Of course, longer reads have extra benefits such as more robust alignments in the presence of polymorphisms or the ability to determine the length of longer repeat polymorphisms. The power-law function also indicates that the reduction of non-specific, difficult-to-align reads with longer read length is not linear.

If we assume our fitting function can be extrapolated to larger k 's for which a direct analysis of k -mer frequencies is restricted by computational constraints, the proportion of non-singleton reads can be predicted. For example, this leads to the prediction of a 0.2% non-singleton rate at the 10kb read length.

It is known that repetitive sequences such as transposable elements and heterochromatin sequences create considerable obstacle in NGS alignment (41). Though transposable elements may exhibit subtle correlation with functional units in the genome (42), it is generally assumed that their biological role is indirect. Accordingly, we also looked at the non-singleton k -mer percentages in RepeatMasker filtered sequences (Figure 1). As expected, the percentage of uniquely mappable sequence is much higher than that in the all-inclusive sequence for short k -mers (e.g. $k < 100$). Interestingly, the differences between the two disappear for longer k -mers (e.g. $k=500$). A note of caution is that 89% of these RepeatMasker-filtered subsequences are shorter than 1kb, making the statistics less reliable at longer k 's.

Maximum k -mer frequency decreases with k slowly

Another measure of the level of redundancy at length scale k is the maximum frequency ($\max(f)$) of k -mer types. For example, base A/T homopolymers of length 20 appear most often with 898647 copies; at $k=400$, AT repeats have more copy numbers ($f=150$) than other 400-mers; the $\max(f)$ for $k=1000$ is equal to 24 for a sequence which is not filtered by the RepeatMasker. The $\max(f)$ as a function of k is shown in Figure 2 in log-log scale.

For RepeatMasker-filtered sequences, $\max(f)$ quickly decays below 100 and then falls only slowly, indicating that RepeatMasker usually finds shorter repeats. At $k=200-500$, the k -mer with the $\max(f) \sim 50$ is a low-complexity sequence, with internal repeats of GGGGGGAACAGC-GACAC/GTGTCCGCTGTTCCCCC. Despite its high prevalence, this low-complexity sequence is not masked by RepeatMasker in the human reference genome.

Fitting of the linear regression, $\log_{10} \max(f) = a + b \log_{10} k$ (or $\log \max(f) \sim \log k$), leads to $(a, b) = (8.99, -2.62)$. Extrapolating this regression to longer k 's predicts that at $k=2724$, $\max(f)=1$. This prediction should be viewed with caution as $\max(f)$ is mainly determined by "outlier" events thus un-reproducible in principle.

Frequency distributions at fixed k values exhibit power-law-like trend: The frequency distribution (FD) describes the distribution of k -mer types according their copy numbers in the genome. When plotted in log-log scale, low-frequent k -mer types and the less redundant portion of the sequence are highlighted. Figure 3 shows five FDs at $k=30, 50, 150, 500$, and 1000 in log-log scale. The FDs at $k=30$ and 50 span a wider frequency range, and the power-law trend is obvious.

A similar FD for $k=40$ in human genome was shown in (43, 44), and a slope of -2.3 in linear regression (in log-log scale) in the $f=3-500$ range was reported. When we fit the $k=50$ FD by linear regression in log-log scale, a very similar fitting slope value is obtained (-2.38 , for $f=3-200$). However, it is clear from Figure 3 that the slopes are steeper for $k=150$ (-2.7 for $f=2-100$), $k=500$ (-3.5 for $f=2-40$), and $k=1000$ (-5.3 for $f=2-19$, or -5.9 from $f=2-9$), indicating that the slope is not a universal parameter.

From the short read alignment perspective, the long tail at the high copy-numbers shows that many sequences cannot be uniquely mapped at smaller k values (e.g. $k=30, 50$). However,

the tail is much shortened at $k=1000$. As expected, the tail for RepeatMasker-filtered sequences at various k values are much shorter (Figure 3, grey lines).

Rank-frequency distributions at fixed k values mostly follows a concave curve in log-log scale

Although rank-frequency distributions (RFD's) can be converted to cumulative FD (36), in log-log scale, it zooms in the high-frequency tail of the frequency distribution. Figure 4 shows five RFD at k 's from 30 to 1000. While the RFD at $k=30$ may maintain a power-law or piecewise power-law trend, those at larger k values become more concave. This concave Zipf's curve is commonly observed in city size distributions (45, 46).

For RFDs deviating from the Zipf's law, functions with two parameters may be used to account for the concave or convex shape of the curve in log-log scale (36). We found that the quadratic logarithmic function, but not the Weibull function, fits the RFDs well (Figure 5). The Beta rank function usually exhibit "S" shapes (39), whereas the RFD in Figure 4 shows a "Z" shape. This motivated us to use a novel reverse Beta function to fit the data (Figure 5). The "Z" shaped log-log RFD means that if the power-law function is the default functional relationship between frequency and rank, frequencies of the intermediately-ranked k -mers decrease faster than the two tails. The "S" shaped log-log RFD implies the opposite.

Mapping $f \geq 10$ 1000-mer to the reference genome

For $k=1000$, there are 6107 k -mer types with frequency f larger or equal to 10. Due to the fact that these are overlapping k -mers, they are mapped to only 172 chromosomal regions, each of a few kb (the 172 locations, number of high-frequency 1000-mers, and the distance from the previous chromosome regions are included in Supplementary Table S1).

A total of 70 out of these 172 regions (or 40%) are clustered in four larger stretches on chromosomes 1 and X and contain long tandem repeats (60, 70 kbase on chromosome 1q21.1, 1q21.2, and 41, 56 kbases on Xq23, Xq24). The two stretches on chromosome 1 contain copies of the neuroblastoma breakpoint family genes (NBPF) (47–49). The Xq24 region contains cancer/testis antigen family genes (CT47A) (50, 51), whereas the Xq23 region has no genes,

but contains the macrosatellite DXZ4 (52–54) which exhibits periodic appearance of other functional elements, such as H3K27Ac or H3K4me2 (55) histone modification marks.

Besides these long stretches, 39 out of 172 regions (or 23%) overlap with 34 genes: *ZNF3850*, *EPHA3*, *COL6A6*, *CD38*, *KCNIP4*, *FRAS1*, *ANTXR2*, *HSD17B11*, *FAM190A*, *DKK2*, *FBXL7*, *AK123816*, *FAM153A*, *FAM65B*, *LAMA2*, *MYCT1*, *NOD1*, *TPST1*, *PSD3*, *KCNB2*, *NR4A3*, *C9orf171*, *CACNA1B*, *DLG2*, *CCDC67*, *UACA*, *HOMER2*, *SMG1*, *CDH13*, *PRKCA*, *LILRA2*, *TTC28*, *MTMR8*, and *SLC25A43*. Obtaining high quality data on genetic variants in these gene sequences is therefore likely to remain a challenge even with longer reads.

DISCUSSION

Long k -mers in the reference genome as surrogate for sequencing reads: The k -mer distribution has many application in sequence analysis, such as measuring similarity between two genomes (56), correcting sequencing error (57), finding repeat structures (58), determining the feasibility of gene patents (59). In many applications, only short k -mers are considered to be relevant, such as $k = 6$ (60), $k \leq 7$ (61), $k=8$ (62), $k=11$ (63). This paper essentially uses long k -mers taken from the reference genome as surrogate for reads from future NGS technologies. Computationally speaking, counting long k -mers is more challenging and we are not aware of any prior publications on the long k -mer distributions in the human genome for k as long as 1000.

As compared to other papers on mappability of genome sequencing reads (3, 5), our more theoretical approach has the advantage of being able to discuss long reads (e.g. $k=1000$) where such data is not available from the current NGS technology. Our approach also separates the two causes of the unmappability: one due to the unfinished sequence in the reference genome and another due to the redundancy in the finished sequences. The unfinished bases are mainly located in the centromeres, short arms of acrocentric chromosomes and other heterochromatic regions, and rich in repetitive sequences. If we always treat this unfinished sequences (total 234 Mbases) to be non-singletons regardless of k , p_{ns} would flatten out around 0.1 (see Figure 1).

A baseline knowledge of redundancy of the human genome at length k level:

Figures 1-3 provides a baseline knowledge of the redundancy of the human genome at the k -mer level. Our results give a more quantitative description on the effect of read length k on the mappability of reads from the finished region of the human genome.

Reference assembly is easier than *de novo* assembly, and our approach does not directly apply to *de novo* sequencing “assemblability”. However the mappability in reference assembly and assemblability in *de novo* assembly are closely related, as repetitive sequences cause problems in both situations (64). The current *de novo* assemblies still do not perform consistently (65, 66) and a quantitative assessment of the impact of repetitive sequences on reference assembly could be a useful piece of information for *de novo* assembly as well. Note that some discussion on k -mer-based assembly actually refers to k' -mer ($k' \ll k$) (67, 68).

Highly redundant regions at $k = 1000$ level and copy-number-variation regions:

The chromosome 1 and X regions which we have identified by showing at least 10 copy numbers of 1000-mers are discussed in the literature as regions with common copy-number-variations (CNV). CNV in the 1q21.1 region, if not NBPF-specific, has been linked to congenital cardiac defect (69–71), autism (72, 73), mental retardation (74), developmental abnormalities (75), schizophrenia (76, 77), and neuroblastoma (78). With so many abnormalities mapped to this region, these are collectively called the chromosome 1q21.1 duplication syndrome in the Online Mendelian Inheritance in Man (OMIM 612475).

The Xq23 region, if not macrosatellite DXZ4 specific, has been identified as likely CNV regions linked to developmental and behavioral problems (79). Chromatin configuration at DXZ4 region is reported to differ between male melanoma cells and normal skin cells (80). The Xq24 region if not the CT47A gene is listed as a candidate CNV region for intellectual disability (81), mental retardation (82), etc.

A well-known mechanism for CNV formation is the non-allelic homologous recombinations (NAHR) between repetitive elements (83). More copies of a repetitive sequence give more opportunities that NAHR could occur, resulting in a natural connection between repetitive sequences and common CNV. The fact that simple counting of 1000-mer frequencies leads to CNV regions with medical implications indicates that understanding the k -mer distribution is an important part of genomic analyses.

Long-tails and the diminishing return of longer reads: Our analysis shows that all

distributions discussed in this paper are better viewed in log-log scale, proving the existence of power-law distributions or long-tails. This has been observed in the past for other genomic distributions, such as correlation function (84–87), power spectrum of base composition (88–91), frequency distribution of gene or protein family size (92–95), sizes of ultraconserved regions (96), and in models with duplications (97–100). Ongoing duplications increase the copy number geometrically, which explains the presence of long-tails.

A consequence of the long-tail in Figure 1 is that with increasing read (or k -mer) lengths, the proportion of reads that cannot be mapped to a unique genomic region (within the finished sequences) decreases algebraically, as compared to linearly or exponentially. Numerically, if not economically, this defines a diminishing return. To assess the economic return with NGS technology with longer reads, other factors should be considered, such as the choice of less redundant target regions such as exome (101), the choice of pair-end sequencing technologies (102) which effectively increases the read length (103) though the mappability may not necessarily improve over the single-end sequencing (4), and the overall cost of longer-read sequencing. Anticipating the eventual high-quality human genome sequences obtained by a combination of various technologies, the k -mer distribution will be a prominent factor determining how these technologies are optimally combined.

SUPPLEMENTARY DATA

Supplementary Data are available at NAR online, including Supplementary Table S1: 172 chromosome locations with high-frequency ($f \geq 10$) 1000-mers.

ACKNOWLEDGEMENTS

We would like to thank Oliver Clay, Andrew Shih, Astero Provata, Yannis Almirantis for discussions, and the authors of DSK for timely responding to our inquiries and fixing bugs. WL and JF acknowledge the support from the Robert S Boas Center for Genomics and Human Genetics.

References

- [1] Rozowsky J, Euskirchen G, Auerbach RK, Zhang ZD, Gibson T, Bjornson R, Carriero N, Snyder M, Gerstein MB (2009) PeakSeq enables systematic scoring of ChIP-seq experiments relative to controls. *Nature Biotech.*, **27**, 66-75.
- [2] Cahill MJ, Köser CU, Ross NE, Archer JAC (2010) Read length and repeat resolution: exploring prokaryote genomes using next-generation sequencing technologies. *PLoS ONE*, **5**, e11518.
- [3] Koehler R, Issac H, Cloonan N, Grimmond SM (2011) The uniqueome: a mappability resource for short-tag sequencing. *Bioinfo.*, **27**, 272-274.
- [4] Derrien T, Estellé J, Marco Sola M, Knowles DG, Raineri E, Guigó R, Ribeca P (2012) Fast computation and applications of genome mappability. *PLoS ONE*, **7**, e30377.
- [5] Lee H, Schatz MC (2012) Genomic dark matter: the reliability of short read mapping illustrated by the genome mappability score. *Bioinfo.*, **28**, 2097-2105.
- [6] Storvall H, Ramsköld D, Sandberg R (2013) Efficient and comprehensive representation of uniqueness for next-Generation sequencing by minimum unique length analyses. *PLoS ONE*, **8**, e53822.
- [7] Weber JL, Myers EW (1997) Human whole-genome shotgun sequencing. *Genome Res.*, **7**, 401-409.
- [8] Green ED (2001) Strategies for the systematic sequencing of complex genomes. *Nature Rev. Genet.*, **2**, 573-583.
- [9] Cheung J, Estivill X, Khaja R, MacDonald JR, Lau K, Tsui LC, Scherer SW (2003) Genome-wide detection of segmental duplications and potential assembly errors in the human genome sequence. *Genome Biol.*, **4**, R25.
- [10] Fraenkel AS, Gillis J (1966) Appendix II. Proof that sequences of A, C, G, and T can be assembled to produce chains of ultimate length avoiding repetitions everywhere. *Prog. Nucl. Acids Res. and Mol. Biol.*, **5**, 343-348.
- [11] Stoppa-Lyonnet D, Carter PE, Meo T, Tosi M (1990) Clusters of intragenic Alu repeats predispose the human C1 inhibitor locus to deleterious rearrangements. *Proc. Natl. Acad. Sci.*, **87**, 1551-1555.
- [12] Conrad B, Antonarakis SE (2007) Gene duplication: a drive for phenotypic diversity and cause of human disease. *Ann. Rev. Genomics and Hum. Genet.*, **8**, 17-35.
- [13] Ohno S (1970) *Evolution by Gene Duplication* (Springer-Verlag).

- [14] Nowak MA, Boerlijst, Cooke J, Maynard Smith J (1997) Evolution of genetic redundancy. *Nature*, **388**, 167-171.
- [15] Fortna A, Kim Y, MacLaren E, Marshall K, Hahn G, Meltesen L, Brenton M, Hink R, Burgers S, Hernandez-Boussard T, Karimpour-Fard A, Glueck D, McGavran L, Berry R, Pollack J, Sikela JM (2004) Lineage-specific gene duplication and loss in human and great ape evolution. *PLoS Biol.*, **2**, E207.
- [16] Krakauer DC, Plotkin JB (2002) Redundancy, antiredundancy, and the robustness of genomes. *Proc. Natl. Acad. Sci.*, **99**, 1405-1409.
- [17] Marcotte EM, Pellegrini M, Yeates TO, Eisenberg D (1998) A census of protein repeats. *J. Mol. Biol.*, **293**, 151-160.
- [18] Liu L, Li Y, Li S, Hu N, He Y, Pong R, Lin D, Lu L, Law M (2012b) Comparison of next-generation sequencing systems. *J. Biomed. Biotech.*, **2012**, 251364.
- [19] Eisenstein M (2013) Companies 'going long' generate sequencing buzz at Marco island (news). *Nature Biotech.*, **31**, 265-266.
- [20] Brown PF, deSouza PV, Mercer RL, Pietra VJ, Lao JC (1992) Class-based n-gram models of natural languages. *J. Comp. Linguistics*, **18**, 467-479.
- [21] Baayen RH (2001) *Word Frequency Distribution* (Kluwer Academic).
- [22] Phoophakdee B (2007) *TRELLIS: genome-size disk-based suffix tree indexing algorithm* (Ph.D Thesis, Rensselaer Polytechnic Institute).
- [23] Phoophakdee B, Zaki MJ (2008) TRELLIS+: an effective approach for indexing genome-scale sequences using suffix trees. *Pacif. Sym. Biocomp.*, **2008**, 90-101.
- [24] Li Q, Yu C, Li Y, Lam TW, Y SM, Kristiansen K, Wang J (2009) SOAP2: an improved ultrafast tool for short read alignment. *Bioinfo.*, **25**, 1966-1967.
- [25] Chu HT, Hsiao WWL, Tsao TT, Hsu DF, Chen CC, Lee SA, Kao CY (2013) SeqEntropy: genome-wide assessment of repeats for short read sequencing. *PLoS ONE*, **8**, e59484.
- [26] Rizk G, Lavenier D, Chikhi R (2013) DSK, k-mer counting with very low memory usage. *Bioinfo.*, **29**, 652-653.
- [27] Kurtz S, Narechania A, Stein JC, Ware D (2008) A new method to compute K-mer frequencies and its application to annotate large repetitive plant genomes. *BMC Genomics*, **9**, 517.

- [28] Marçais G, Kingsford C (2011) A fast, lock-free approach for efficient parallel counting of occurrences of k-mers. *Bioinfo.*, **27**, 764-770.
- [29] Melsted P, Pritchard JK (2011) Efficient counting of k-mers in DNA sequences using a bloom filter. *BMC Bioinfo.*, **12**, 333.
- [30] Anderson C (2006) *The Long Tail: Why the Future of Business is Selling Less of More* (Hyperion).
- [31] Clauset A, Shalizi CR, Newman MEJ (2007) Power-law distributions in empirical data. *SIAM Rev.*, **51**, 661-703.
- [32] Zipf GK (1949) *Human Behavior and the Principle of Least Effort* (Addison-Wesley).
- [33] Sharp AJ, Locke DP, McGrath SD, Cheng Z, Bailey JA, Vallente RU, Pertz LM, Clark RA, Schwartz S, Segreaves R, Oseroff VV, Albertson DG, Pinkel D, Eichler EE (2005) Segmental duplications and copy-number variation in the human genome. *Am. J. Hum. Genet.*, **77**, 78-88.
- [34] Perry GH, Tchinda J, McGrath SD, Zhang J, Picker SR, Cáceres AM, Iafrate AJ, Tyler-Smith C, Scherer SW, Eichler EE, Stone AC, Lee C (2006) Hotspots for copy number variation in chimpanzees and humans. *Proc. Natl. Acad. Sci.*, **101**, 8006-8011.
- [35] Genovese G, Handsaker RE, Li H, Altemose N, Lindgren AM, Chambert K, Pasaniuc B, Price AL, Reich D, Morton CC, Pollak MR, Wilson JG, McCarroll SA (2013) Using population admixture to help complete maps of the human genome. *Nature Genet.*, **45**, 406-414.
- [36] Li W, Miramontes P, Cocho G (2010) Fitting ranked linguistic data with two-parameter functions. *Entropy*, **12**, 1743-1764.
- [37] Li W, Miramontes P (2011) Fitting ranked English and Spanish letter frequency distribution in US and Mexican presidential speeches. *J. Quant. Linguistics*, **18**, 337-358.
- [38] Mansilla R, Köppen E, Cocho G, Miramontes P (2007) On the behavior of journal impact factor rank-order distribution. *J. Infometrics*, **1**, 155-160.
- [39] Martínez-Mekler G, Alvarez Martínez R, Beltrán del Río M, Mansilla R, Miramontes P, Cocho G (2009) Universality of rank-ordering distributions in the arts and sciences. *PLoS ONE*, **4**, e4791.
- [40] Haubold B, Pierstorff N, Möller F, Wiehe T (2005) Genome comparison without alignment using shortest unique substrings. *BMC Bioinfo.*, **6**, 123.
- [41] Treangen TJ, Salzberg SL (2012) Repetitive DNA and next-generation sequencing: computational challenges and solutions. *Nature Rev. Genet.*, **13**, 36-46.

- [42] Li W, Sosa D, Jose MV (2013) Human repetitive sequence densities are mostly negatively correlated with R/Y-based nucleosome-positioning motifs and positively correlated with W/S-based motifs. *Genomics*, **101**, 125-133.
- [43] Sindi SS (2006) *Describing and Modeling Repetitive Sequences in DNA* (Ph.D Thesis, Univ. of Maryland).
- [44] Sindi SS, Hunt BR, Yorke JA (2008) Duplication count distributions in DNA sequences. *Phys. Rev. E*, **78**, 061912.
- [45] Gabaix X, Ioannides YM (2004) The evolution of city size distributions. in *Handbook of Regional and Urban Economics*, eds. Henderson V, Thisse JF (North-Holland).
- [46] Eeckhout J (2004) Gibrat's law for (all) cities. *Am. Eco. Rev.*, **94**, 1429-1451.
- [47] Vandepoele K, Van Roy N, Staes K, Speleman F, van Roy F (2005) A novel gene family NBPF: intricate structure generated by gene duplications during primate evolution. *Mol. Biol. Evol.* , **22**, 2265-2274.
- [48] Paar V, Glunčić M, Rosandić, Basar I, Vlahović I (2011) Intragene higher order repeats in neuroblastoma breakpoint family genes distinguish humans from chimpanzees. *Mol. Biol. Evol.*, **28**, 1877-1892.
- [49] Dumas LJ, O'Bleness MS, Davis JM, Dickens CM, Anderson N, Keeney JG, Jackson J, Sikela M, Raznahan A, Giedd J, Rapoport J, Nagamani SS, Erez A, Brunetti-Pierri N, Sugalski R, Lupski JR, Fingerlin T, Cheung SW, Sikela JM (2012) DUF1220-domain copy number implicated in human brain-size pathology and evolution. *Am. J. Hum. Genet.*, **91**, 444-454.
- [50] Chen YT, Iseli C, Venditti CA, Old LJ, Simpson AJ, Jongeneel CV (2006) Identification of a new cancer/testis gene family, CT47, among expressed multicopy genes on the human X chromosome. *Genes, Chromosomes & Cancer*, **45**, 392-400,
- [51] Dobrynin P, Matyunina E, Malov SV, Kozlov AP (2013) The novelty of human cancer/testis antigen encoding genes in evolution. *Int. J. Genomics*, **2013**, 105108.
- [52] Giacalone J, Friedes J, Francke U (1992) A novel GC-rich human macrosatellite VNTR in Xq24 is differentially methylated on active and inactive X chromosomes. *Nature Genet.* , **1**, 137-143.
- [53] Tremblay DC, Moseley S, Chadwick BP (2010) Variation in array size, monomer composition and expression of the macrosatellite DXZ4. *PLoS ONE*, **6**, e18969
- [54] Schaap M, Lemmers R, Maassen R, van der Vliet PJ, Hoogerheide LF, van Dijk HK, Batrk N, de Knijff P, van der Maarel SM (2013) Genome-wide analysis of macrosatellite repeat copy number variation in worldwide populations: evidence for differences and commonalities in size distributions and size restrictions. *BMC Genomics*, **14**, 143.

- [55] Horakova AH, Moseley SC, McLaughlin CR, Tremblay DC, Chadwick BP (2012) The macrosatellite DXZ4 mediates CTCF-dependent long-range intrachromosomal interactions on the human inactive X chromosome. *Hum. Mol. Genet.*, **21**, 4367-4377.
- [56] Edgar RC (2004) MUSCLE: a multiple sequence alignment method with reduced time and space complexity. *BMC Bioinfo.*, **5**, 113.
- [57] Liu Y, Schröder J, Schmidt B (2013) Musket: a multistage k-mer spectrum-based error corrector for Illumina sequence data. *Bioinfo.*, **29**, 308-315.
- [58] Li X, Waterman MS (2003) Estimating the repeat structure and length of DNA sequences using l-tuples. *Genome Res.*, **13**, 1916-1922.
- [59] Rosenfeld J, Mason CE (2013) Pervasive sequence patents cover the entire human genome. *Genome Med.*, **5**, 27.
- [60] Chen YH, Nyeo SL, Yeh CY (2005) Model for the distributions of k-mers in DNA sequences. *Phys. Rev. E*, **72**, 011908.
- [61] Nikolaou C, Almirantis Y (2005) 'Word' preference in the genomic text and genome evolution: different modes of n-tuplet usage in coding and noncoding sequences. *J. Mol. Evol.*, **61**, 23-25.
- [62] Xie H, Hao B (2002) Visualization of K-tuple distribution in procaryote complete genomes and their randomized counterparts. *Proc. IEEE Comp. Soc. Conf. on Bioinfo.*, pp.31-42.
- [63] Chor B, Horn D, Goldman N, Levy Y, Massingham T (2009) Genomic DNA k-mer spectra: models and modalities. *Genome Biol.*, **10**, R108.
- [64] Paszkiewicz K, Studholme DJ (2010) *de novo* assembly of short sequence reads. *Brief. Bioinfo.*, **11**, 457-472.
- [65] Bradnam KR, Fass JN, Alexandrov A, Baranay P, Bechner M, Birol I, Boisvert S, Chapman JA, Chapuis G, Chikhi R, Chitsaz H, Chou, WC, Corbeil J, Del Fabbro C, Docking TR, Durbin R, Earl D, Emrich S, Fedotov P, Fonseca NA, Ganapathy G, Gibbs RA, Gnerre S, Godzaridis E, Goldstein S, Haimel M, Hall G, Haussler D, Hiatt JB, Ho IY, Howard J, Hunt M, Jackman SD, Jaffe DB, Jarvis E, Jiang H, Kazakov S, Kersey PJ, Kitzman, JO, Knight JR, Koren S, Lam TW, Lavenier D, Laviolette F, Li Y, Li Z, Liu B, Liu Y, Luo R, MacCallum I, MacManes MD, Maillet N, Melnikov S, Vieira BM, Naquin D, Ning Z, Otto TD, Paten B, Paulo OS, Phillippy AM, Pina-Martins F, Place M, Przybylski D, Qin X, Qu C, Ribeiro FJ, Richards S, Rokhsar DS, Ruby JG, Scalabrin S, Schatz MC, Schwartz DC, Sergushichev A, Sharpe T, Shaw TI, Shendure J, Shi Y, Simpson JT, Song H, Tsarev F, Vezzi F, Vicedomini R, Wang J, Worley KC, Yin S, Yiu SM, Yuan J, Zhang G, Zhang H, Zhou S, Korf IF, (2013) Assemblathon 2: evaluating *de novo* methods of genome assembly in three vertebrate species. arXiv preprint, arXiv:1301.5406.

- [66] Muñoz JF, Gallo JE, Misas E, McEwan JG, Clay OK (2013) The eukaryotic genome, its reads, and the unfinished assembly. *FEBS Lett.*, **587**, 2090-2093.
- [67] Zerbino D, Birney E (2008) Velvet: Algorithms for de novo short read assembly using de Bruijn graphs. *Genome Res.*, **18**, 821-829.
- [68] Liu B, Yuan J, Yiu SM, Li Z, Xie Y, Chen Y, Shi Y, Zhang H, Li Y, Lam TW, Luo R (2012a) COPE: an accurate k-mer-based pair-end reads connection tool to facilitate genome assembly. *Bioinfo.*, **28**, 2870-2874.
- [69] Christiansen J, Dyck JD, Elyas BG, Lilley M, Bamforth JS, Hicks M, Sprysak KA, Tomaszewski R, Haase SM, Vicen-Wyhony LM, Somerville MJ (2004) Chromosome 1q21.1 contiguous gene deletion is associated with congenital heart disease. *Circ. Res.*, **94**, 1429-1435.
- [70] Redon R, Ishikawa S, Fitch KR, Feuk L, Perry GH, Andrews TD, Fiegler H, Shapero MH, Carson AR, Chen W, Cho EK, Dallaire S, Freeman JL, González JR, Gratacós M, Huang J, Kalaitzopoulos D, Komura D, MacDonald JR, Marshall CR, Mei R, Montgomery L, Nishimura K, Okamura K, Shen F, Somerville MJ, Tchinda J, Valsesia A, Woodwark C, Yang F, Zhang J, Zerjal T, Zhang J, Armengol L, Conrad DF, Estivill X, Tyler-Smith C, Carter NP, Aburatani H, Lee C, Jones KW, Scherer SW, Hurles ME (2006) Global variation in copy number in the human genome. *Nature*, **444**, 444-454.
- [71] Greenway SC, Pereira AC, Lin JC, DePalma SR, Israel SJ, Mesquita SM, Ergul E, Conta JH, Korn JM, McCarroll SA, Gorham JM, Gabriel S, Altshuler DM, Quintanilla-Dieck Mde L, Artunduaga MA, Eavey RD, Plenge RM, Shadick NA, Weinblatt ME, De Jager PL, Hafler DA, Breitbart RE, Seidman JG, Seidman CE (2009) *De novo* copy number variants identify new genes and loci in isolated sporadic tetralogy of Fallot. *Nature Genet.*, **41**, 931-935.
- [72] Autism Genome Project Consortium, Szatmari P, Paterson AD, Zwaigenbaum L, Roberts W, Brian J, Liu XQ, Vincent JB, Skaug JL, Thompson AP, Senman L, Feuk L, Qian C, Bryson SE, Jones MB, Marshall CR, Scherer SW, Vieland VJ, Bartlett C, Mangin LV, Goedken R, Segre A, Pericak-Vance MA, Cuccaro ML, Gilbert JR, Wright HH, Abramson RK, Betancur C, Bourgeron T, Gillberg C, Leboyer M, Buxbaum JD, Davis KL, Hollander E, Silverman JM, Hallmayer J, Lotspeich L, Sutcliffe JS, Haines JL, Folstein SE, Piven J, Wassink TH, Sheffield V, Geschwind DH, Bucan M, Brown WT, Cantor RM, Constantino JN, Gilliam TC, Herbert M, Lajonchere C, Ledbetter DH, Lese-Martin C, Miller J, Nelson S, Samango-Sprouse CA, Spence S, State M, Tanzi RE, Coon H, Dawson G, Devlin B, Estes A, Flodman P, Klei L, McMahon WM, Minshew N, Munson J, Korvatska E, Rodier PM, Schellenberg GD, Smith M, Spence MA, Stodgell C, Tepper PG, Wijsman EM, Yu CE, Rogé B, Mantoulan C, Wittmeyer K, Poustka A, Felder B, Klauck SM, Schuster C, Poustka F, Blte S, Feineis-Matthews S, Herbrecht E, Schmötzer G, Tsiantis J, Papanikolaou K, Maestrini E, Bacchelli E, Blasi F, Carone S, Toma C, Van Engeland H, de Jonge M, Kemner C, Koop

- F, Langemeijer M, Hijmans C, Staal WG, Baird G, Bolton PF, Rutter ML, Weisblatt E, Green J, Aldred C, Wilkinson JA, Pickles A, Le Couteur A, Berney T, McConachie H, Bailey AJ, Francis K, Honeyman G, Hutchinson A, Parr JR, Wallace S, Monaco AP, Barnby G, Kobayashi K, Lamb JA, Sousa I, Sykes N, Cook EH, Guter SJ, Leventhal BL, Salt J, Lord C, Corsello C, Hus V, Weeks DE, Volkmar F, Tauber M, Fombonne E, Shih A, Meyer KJ (2007) Mapping autism risk loci using genetic linkage and chromosomal rearrangements. *Nature Genet.*, **39**, 319-328.
- [73] Girirajan S, Dennis MY, Baker C, Malig M, Coe BP, Campbell CD, Mark K, Vu TH, Alkan C, Cheng Z, Biesecker LG, Bernier R, Eichler EE (2013) Refinement and discovery of new hotspots of copy-number variation associated with autism spectrum disorder. *Am. J. Hum. Genet.*, **92**, 221-237.
- [74] Mefford HC, Sharp AJ, Baker C, Itsara A, Jiang Z, Buysse K, Huang S, Maloney VK, Crolla JA, Baralle D, Collins A, Mercer C, Norga K, de Ravel T, Devriendt K, Bongers EM, de Leeuw N, Reardon W, Gimelli S, Bena F, Hennekam RC, Male A, Gaunt L, Clayton-Smith J, Simonic I, Park SM, Mehta SG, Nik-Zainal S, Woods CG, Firth HV, Parkin G, Fichera M, Reitano S, Lo Giudice M, Li KE, Casuga I, Broomer A, Conrad B, Schwerzmann M, Räber L, Gallati S, Striano P, Coppola A, Tolmie JL, Tobias ES, Lilley C, Armengol L, Spyschaert Y, Verloo P, De Coene A, Goossens L, Mortier G, Speleman F, van Binsbergen E, Nelen MR, Hochstenbach R, Poot M, Gallagher L, Gill M, McClellan J, King MC, Regan R, Skinner C, Stevenson RE, Antonarakis SE, Chen C, Estivill X, Menten B, Gimelli G, Gribble S, Schwartz S, Sutcliffe JS, Walsh T, Knight SJ, Sebat J, Romano C, Schwartz CE, Veltman JA, de Vries BB, Vermeesch JR, Barber JC, Willatt L, Tassabehji M, Eichler EE (2008) Recurrent rearrangements of chromosome 1q21.1 and variable pediatric phenotypes. *New Eng. J. Med.*, **359**, 1685-1699.
- [75] Brunetti-Pierri N, Berg JS, Scaglia F, Belmont J, Bacino CA, Sahoo T, Lalani SR, Graham B, Lee B, Shinawi M, Shen J, Kang SH, Pursley A, Lotze T, Kennedy G, Lansky-Shafer S, Weaver C, Roeder ER, Grebe TA, Arnold GL, Hutchison T, Reimschisel T, Amato S, Geraghty MT, Innis JW, Obersztyn E, Nowakowska B, Rosengren SS, Bader PI, Grange DK, Naqvi S, Garnica AD, Bernes SM, Fong CT, Summers A, Walters WD, Lupski JR, Stankiewicz P, Cheung SW, Patel A (2008) Recurrent reciprocal 1q21.1 deletions and duplications associated with microcephaly or macrocephaly and developmental and behavioral abnormalities. *Nature Genet.*, **40**, 1466-1471.
- [76] The International Schizophrenia Consortium (2008) Rare chromosomal deletions and duplications increase risk of schizophrenia. *Nature*, **455**, 237-241.
- [77] Ikeda M, Aleksic B, Kirov G, Kinoshita Y, Yamanouchi Y, Kitajima T, Kawashima K, Okochi T, Kishi T, Zaharieva I, Owen MJ, O'Donovan MC, Ozaki N, Iwata N (2010) Copy number variation in schizophrenia in the Japanese population. *Biol. Psych.*, **67**, 283-286.

- [78] Diskin SJ, Hou C, Glessner JT, Attiyeh EF, Laudenslager M, Bosse K, Cole K, Mossé YP, Wood A, Lynch JE, Pecor K, Diamond M, Winter C, Wang K, Kim C, Geiger EA, McGrady PW, Blakemore AI, London WB, Shaikh TH, Bradfield J, Grant SF, Li H, Devoto M, Rappaport ER, Hakonarson H, Maris JM (2009) Copy number variation at 1q21.1 associated with neuroblastoma. *Nature*, **459**, 987-991.
- [79] Isrie M, Froyen G, Devriendt K, de Ravel T, Fryns JP, Vermeesch JR, Van Esch H (2012) Sporadic male patients with intellectual disability: contribution of X-chromosome copy number variants. *Euro. J. Med. Genet.*, **55**, 577-585.
- [80] Moseley SC, Rizkallah R, Tremblay DC, Anderson BR, Hurt MM, Chadwick BP (2012) YY1 associates with the macrosatellite DXZ4 on the inactive X chromosome and binds with CTCF to a hypomethylated form in some male carcinomas. *Nucl. Acids Res.*, **40**, 1596-1608.
- [81] Whibley AC, Plagnol V, Tarpay PS, Abidi F, Fullston T, Choma MK, Boucher CA, Shepherd L, Willatt L, Parkin G, Smith R, Futreal PA, Shaw M, Boyle J, Licata A, Skinner C, Stevenson RE, Turner G, Field M, Hackett A, Schwartz CE, Gecz J, Stratton MR, Raymond FL (2010) Fine-scale survey of X chromosome copy number variants and indels underlying intellectual disability. *Am. J. Hum. Genet.*, **87**, 173-188.
- [82] Honda S, Hayashi S, Imoto I, Toyama J, Okazawa H, Nakagawa E, Goto Y, Inazawa J (2010) Copy-number variations on the X chromosome in Japanese patients with mental retardation detected by array-based comparative genomic hybridization analysis. *J. Hum. Genet.*, **55**, 590-599.
- [83] Gu W, Zhang F, Lupski JR (2008) Mechanisms for human genomic rearrangement. *PathoGenet.*, **1**, 4.
- [84] Li W, Kaneko K (1992) Long-range correlation and partial $1/f^\alpha$ spectrum in a noncoding DNA sequence. *Europhys. Lett.*, **17**, 655-660.
- [85] Li W (1997) The study of correlation structures of DNA sequences: a critical review. *Comput. Chem.*, **21**, 257-271.
- [86] Bernaola-Galván P, Carpena P, Román-Roldán R, Oliver JL (2002) Study of statistical correlations in DNA sequences. *Gene*, **300**, 105-115.
- [87] Arneodo A, Vaillant C, Audit B, Argoul F, d'Aubenton-Carafa Y, Thermes C (2011) Multi-scale coding of genomic information: from DNA sequence to genome structure and function. *Phys. Rep.*, **498**, 45-188.
- [88] Voss RF (1992) Evolution of long-range fractal correlations and $1/f$ noise in DNA base sequences. *Phys. Rev. Lett.*, **68**, 3805-3808.
- [89] Fukushima A, Ikemura T, Kinouchi M, Oshima T, Kudo Y, Mori H, Kanaya S (2002) Periodicity in prokaryotic and eukaryotic genomes identified by power spectrum analysis. *Gene*, **300**, 203-211.

- [90] Li W, Holste D (2004) Spectral analysis of guanine and cytosine fluctuations of mouse genomic DNA. *Fluc. Noise Lett.*, **4**, L453-L464.
- [91] Li W, Holste D (2005) Universal $1/f$ noise, crossovers of scaling exponents, and chromosome-specific patterns of guanine-cytosine content in DNA sequences of the human genome. *Phys. Rev. E*, **71**, 041910.
- [92] Huynen M, van Nimwegen E (1998) The frequency distribution of gene family sizes in complete genomes. *Mol. Biol. and Evol.*, **15**, 583-589.
- [93] Qian J, Luscombe NM, Gerstein M (2001) Protein family and fold occurrence in genomes: power-law behaviour and evolutionary model. *J. Mol. Biol.*, **313**, 673-681.
- [94] Koonin EV (2011) Are there laws of genome evolution? *PLoS Comp. Biol.*, **7**, e1002173.
- [95] Herrada A, Euíluz VM, Hernández-García E, Duarte CM (2011) Scaling properties of protein family phylogenies. *BMC Evol. Biol.*, **11**, 155.
- [96] Salerno W, Havlak P, Miller J (2006) Scale-invariant structure of strongly conserved sequence in genomic intersections and alignments. *Proc. Natl. Acad. Sci.*, **103**, 13121-13125.
- [97] Li W (1991) Expansion-modification systems: a model for spatial $1/f$ spectra. *Phys. Rev. A*, **43**, 5240-5260.
- [98] Yanai I, Camacho CJ, DeLisi C (2000) Predictions of gene family distributions in microbial genomes: evolution by gene duplication and modification. *Phys. Rev. Lett.*, **85**, 2641-2644.
- [99] Teichmann SA, Babu MM (2004) Gene regulatory network growth by duplication. *Nature Genet.*, **36**, 492-496.
- [100] Massip F, Arndt PF (2013) Neutral evolution of duplicated DNA: an evolutionary stick-breaking process causes scale-invariant behavior. *Phys. Rev. Lett.*, **110**, 148101.
- [101] Ng SB, Turner EH, Robertson PD, Flygare SD, Bigham AW, Lee C, Shaffer T, Wong M, Bhattacharjee A, Eichler EE, Bamshad M, Nickerson DA, Shendure J (2009) Targeted capture and massively parallel sequencing of 12 human exome. *Nature*, **461**, 272-276.
- [102] Korbel JO, Urban AE, Affourtit JP, Godwin B, Grubert F, Simons JF, Kim PM, Palejev D, Carriero NJ, Du L, Taillon BE, Chen Z, Tanzer A, Saunders AC, Chi J, Yang F, Carter NP, Hurler ME, Weissman SM, Harkins TT, Gerstein MB, Egholm M, Snyder M (2007) Paired-end mapping reveals extensive structural variation in the human genome. *Science*, **318**, 420-426.
- [103] Ramachandran P, Palidwor GA, Porter CJ, Perkins TJ (2013) MaSC: mappability-sensitive cross-correlation for estimating mean fragment length of single-end short-read sequencing data. *Bioinfo.*, **29**, 444-450.

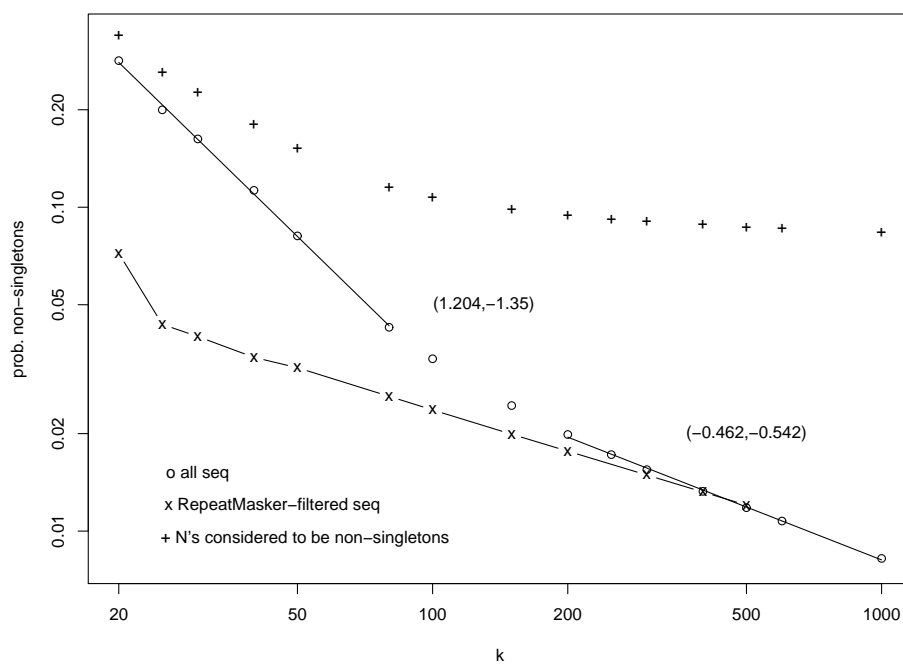


Figure 1: Proportion of non-singleton k -mers/tokens in the human genome (24 chromosomes) as a function of k (in log-log scale). Circles (o) show the results for all finished basepairs, whereas crosses (x) for the result from RepeatMasker-filtered sequences. Pluses (+) are results when unfinished sequences (234 Mbase) are included as non-singletons.

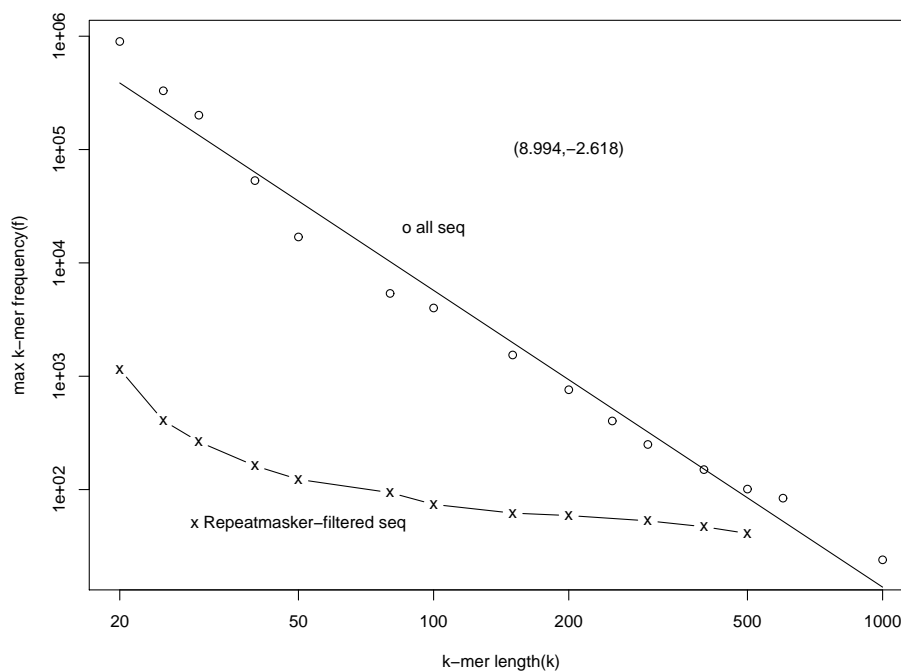


Figure 2: Maximum frequencies of k -mers as a function of k (in log-log scale). Circles (o) show the results for all finished bases, whereas crosses (x) for the result from RepeatMasker-filtered bases.

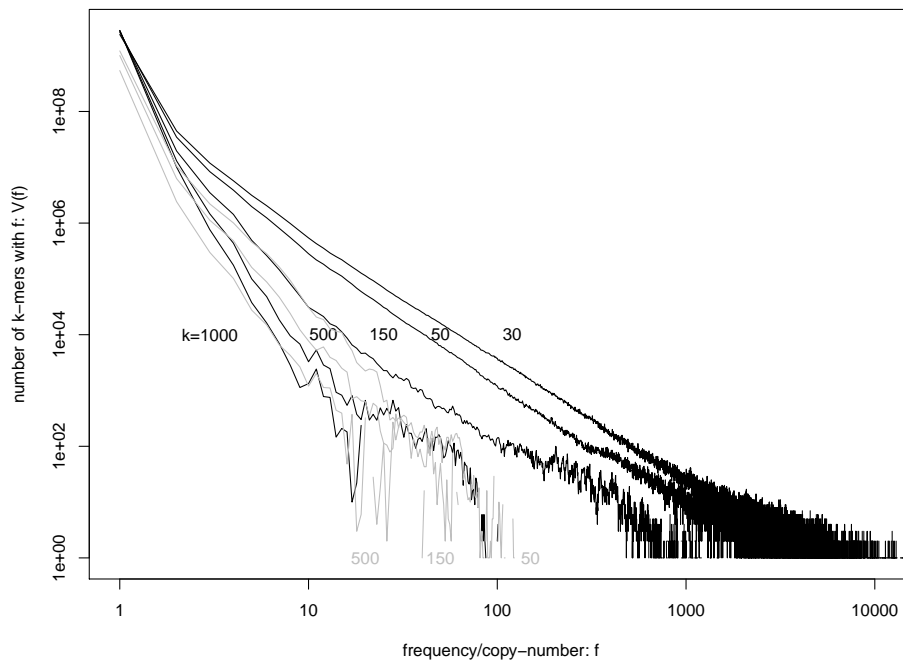


Figure 3: Frequency distributions of k -mers at $k=30, 50, 150, 500$, and 1000 (in log-log scale). The distributions for k -mers in repeat-filtered sequences at $k=50, 150, 500$ are shown in grey lines.

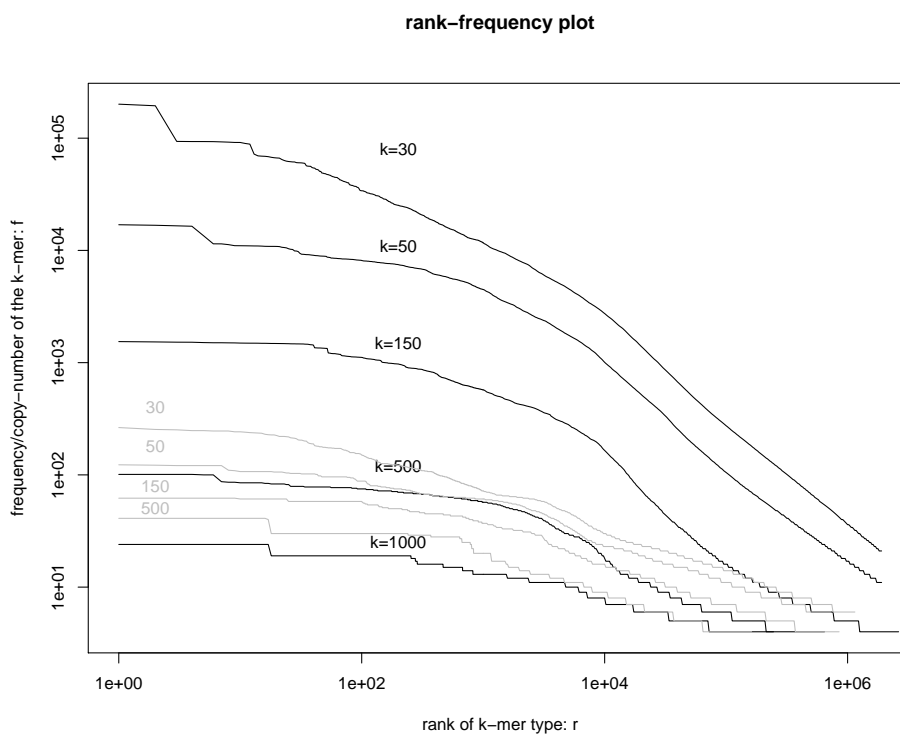


Figure 4: Rank-frequency distributions for k -mers at $k= 30, 50, 150, 500,$ and 1000 (in log-log scale). The corresponding rank-frequency distributions for RepeatMasker-filtered sequences at $k= 30, 50, 150, 500$ are shown in grey lines.

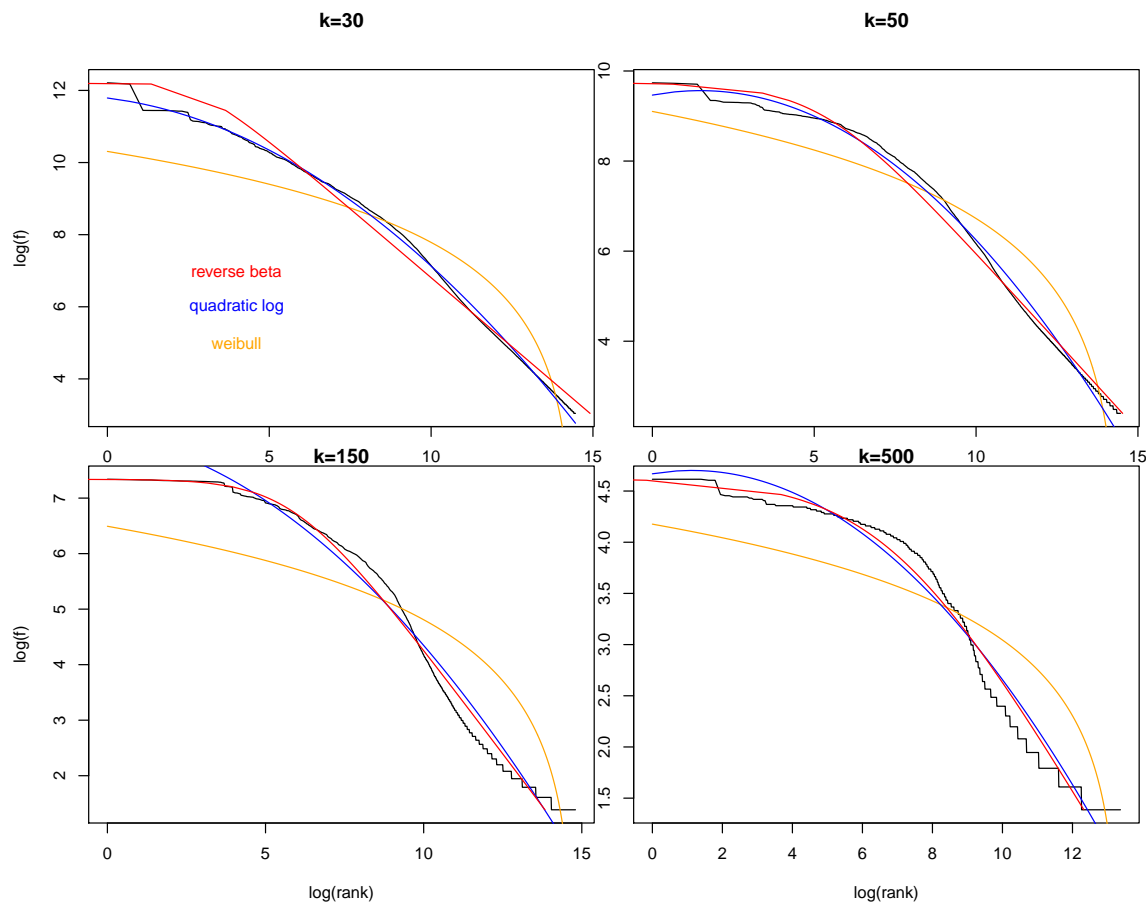


Figure 5: Fitting rank-frequency distribution of k -mers at $k=30, 50, 150, 500$ using three functions. Red: quadratic logarithmic ($\log f \sim \log(r) + \log((r))^2$, f : frequency of a k -mer type, r : rank of a k -mer type, and the \sim symbol represents linear regression); blue: reverse Beta rank function ($\log(r) \sim \log(f) + \log(\max(f) + 1 - f)$); Orange: Weibull function ($\log(f) \sim \log(\log((\max(r) + 1)/r))$).

Supplementary material: Table S1

Chromosome locations of $k=1000$ -mers with frequency $f \geq 10$ mapped to the human reference genome (GRCh37/hg19, Feb 2009). The seven columns are: 1. chromosome (23 for chromosome X); 2. starting position (in base); 3. ending position (in base); 4. width of the region (in kbases); 5. number of 1000-mers mapped to this region; 6. spacing with the previous region (in base); 7 (if available) gene name.

ch	start	end	width(kb)	num-entity	dist-prev-end	gene-name
1	56831364	56833043	1.679	390	56831364	
1	84518510	84519720	1.210	162	27685467	
1	84521988	84523534	1.546	333	2268	
1	144163689	144164940	1.251	253	59640155	NBPF-family

1	144164949	144166172	1.223	156	9	NBPF-family
1	144166529	144168209	1.680	682	357	NBPF-family
1	144171267	144172868	1.601	603	3058	NBPF-family
1	144174458	144177621	3.163	1238	1590	NBPF-family
1	144178038	144179323	1.285	287	417	NBPF-family
1	144179746	144180804	1.058	60	423	NBPF-family
1	144180830	144184012	3.182	710	26	NBPF-family
1	144190348	144193522	3.174	961	6336	NBPF-family
1	144193538	144195088	1.550	552	16	NBPF-family
1	144195507	144201554	6.047	1426	419	NBPF-family
1	144203065	144204372	1.307	264	1511	NBPF-family
1	144206755	144207807	1.052	54	2383	NBPF-family
1	144207827	144209509	1.682	684	20	NBPF-family
1	144211012	144214175	3.163	1238	1503	NBPF-family
1	144214195	144215877	1.682	684	20	NBPF-family
1	144217378	144220552	3.174	961	1501	NBPF-family
1	144222542	144223699	1.157	154	1990	NBPF-family
1	148255552	148256803	1.251	253	4031853	NBPF-family
1	148257416	148258725	1.309	260	613	NBPF-family
1	148260316	148261567	1.251	253	1591	NBPF-family
1	148263509	148265059	1.550	552	1942	NBPF-family
1	148265073	148268247	3.174	710	14	NBPF-family
1	148268281	148269831	1.550	552	34	NBPF-family
1	148271714	148273021	1.307	264	1883	NBPF-family
1	148273051	148277793	4.742	1139	30	NBPF-family
1	148278120	148280976	2.856	931	327	NBPF-family
1	148282487	148284169	1.682	684	1511	NBPF-family
1	148285680	148286965	1.285	287	1511	NBPF-family
1	148287392	148288944	1.552	554	427	NBPF-family
1	148288961	148291735	2.774	563	17	NBPF-family
1	148292162	148293714	1.552	554	427	NBPF-family
1	148293731	148296505	2.774	563	17	NBPF-family
1	148296932	148298484	1.552	554	427	NBPF-family
1	148298501	148301275	2.774	561	17	NBPF-family
1	148301694	148303244	1.550	552	419	NBPF-family
1	148303258	148306035	2.777	311	14	NBPF-family
1	148308035	148309286	1.251	253	2000	NBPF-family

1	148311228	148312780	1.552	554	1942	NBPF-family
1	148312794	148315968	3.174	963	14	NBPF-family
1	148317640	148318820	1.180	101	1672	NBPF-family
1	148320748	148322300	1.552	554	1928	NBPF-family
1	148322314	148325488	3.174	708	14	NBPF-family
1	237186076	237187264	1.188	15	88860588	
1	247852722	247854662	1.940	370	10665458	
2	4782957	4784039	1.082	68	NA	
2	11138506	11139623	1.117	51	6354467	
2	134968954	134970563	1.609	162	123829331	
3	22092360	22093571	1.211	63	NA	ZNF3850
3	22096119	22097785	1.666	577	2548	ZNF3850
3	80925499	80926606	1.107	34	58827714	
3	89513287	89515334	2.047	638	8586681	EPHA3
3	108920256	108921439	1.183	93	19404922	
3	130351657	130352915	1.258	260	21430218	COL6A6
3	137072367	137073449	1.082	84	6719452	
4	15845170	15846306	1.136	138	NA	CD38
4	21163013	21164348	1.335	237	5316707	KCNIP4
4	21165563	21167050	1.487	448	1215	KCNIP4
4	71194736	71195804	1.068	40	50027686	
4	75644610	75646550	1.940	370	4448806	
4	79271909	79273254	1.345	73	3625359	FRAS1
4	80863626	80864733	1.107	34	1590372	ANTXR2
4	80890063	80891544	1.481	131	25330	
4	88268648	88269936	1.288	210	7377104	HSD17B11
4	88270964	88272227	1.263	165	1028	HSD17B11
4	88272229	88273386	1.157	159	2	HSD17B11
4	91600685	91602074	1.389	147	3327299	FAM190A
4	108005014	108277809	272.795	128	16402940	DKK2
4	137214667	137216333	1.666	577	28936858	
4	137217568	137220031	2.463	776	1235	
4	139471548	139473214	1.666	577	2251517	
5	10479	11579	1.100	60	NA	
5	15906794	15907818	1.024	26	15895215	FBXL7
5	57682240	57683559	1.319	49	41774422	
5	103855313	103857622	2.309	547	46171754	

5	108595761	108598576	2.815	772	4738139	
5	152268410	152269605	1.195	120	43669834	AK123816
5	166395979	166397375	1.396	381	14126374	
5	177201688	177203367	1.679	390	10804313	FAM153A
5	177203999	177205005	1.006	8	632	FAM153A
6	24814196	24815833	1.637	335	NA	
6	24816124	24817135	1.011	13	291	
6	86712093	86713844	1.751	383	61894958	
6	129321768	129322865	1.097	99	42607924	LAMA2
6	133342240	133343397	1.157	141	4019375	
6	133344551	133346228	1.677	285	1154	
6	153032481	153033556	1.075	77	19686253	MYCT1
7	30481972	30482979	1.007	9	NA	NOD1
7	32390477	32392004	1.527	176	1907498	
7	49720296	49721702	1.406	7	17328292	
7	49723677	49725225	1.548	525	1975	
7	65756060	65757315	1.255	41	16030835	TPST1
7	96479274	96481321	2.047	638	30721959	
7	113416172	113417537	1.365	367	16934851	
7	141620623	141622142	1.519	419	28203086	
8	73787961	73789068	1.107	34	55332129	KCNB2
8	126597079	126598414	1.335	237	52808011	
8	126599450	126600465	1.015	17	1036	
8	129468131	129469267	1.136	138	2867666	
8	129469381	129470594	1.213	215	114	
8	135086298	135087380	1.082	68	5615704	
8	18454681	18455832	1.151	153	NA	PSD3
9	96880037	96881079	1.042	44	NA	
9	98464614	98465721	1.107	34	1583535	
9	102615779	102616803	1.024	26	4150058	NR4A3
9	135401989	135402996	1.007	9	32785186	C9orf171
9	140912461	140914051	1.590	592	5509465	CACNA1B
10	107137274	107138381	1.107	34	NA	
10	111574095	111575101	1.006	8	4435714	
11	24351213	24352216	1.003	5	NA	
11	24354168	24355533	1.365	367	1952	
11	60852454	60853848	1.394	373	36496921	

11	85038244	85039346	1.102	104	24184396	DLG2
11	93155588	93156702	1.114	42	8116242	CCDC67
11	93158897	93160004	1.107	34	2195	CCDC67
11	95170052	95171840	1.788	545	2010048	
11	95173750	95175002	1.252	204	1910	
11	125410876	125411942	1.066	68	30235874	
12	75271094	75272762	1.668	318	NA	
12	88141507	88142614	1.107	34	12868745	
12	126784020	126785217	1.197	149	38641406	
12	126787028	126788915	1.887	570	1811	
13	30220115	30221202	1.087	89	NA	
14	63587645	63588655	1.010	12	NA	
15	55220178	55221857	1.679	390	NA	
15	71023909	71025588	1.679	390	15802052	UACA
15	83555788	83556968	1.180	182	12530200	HOMER2
16	236025	237244	1.219	200	NA	
16	16936305	16937984	1.679	390	16699061	
16	18834487	18836369	1.882	489	1896503	SMG1
16	83671524	83673049	1.525	174	64835155	CDH13
17	64594609	64595616	1.007	9	NA	PRKCA
17	68457097	68458432	1.335	237	3861481	
17	68459468	68461134	1.666	577	1036	
18	68415980	68417774	1.794	319	NA	
19	55091938	55092944	1.006	8	NA	LILRA2
22	29064027	29065134	1.107	34	NA	TTC28
23	11730147	11731404	1.257	259	NA	
23	11957210	11958761	1.551	528	225806	
23	63474347	63475805	1.458	33	51515586	MTMR8
23	81101312	81102523	1.211	202	17625507	
23	114959682	114961907	2.225	1227	33857159	macrosatellite-DXZ4
23	114962577	114964888	2.311	1313	670	macrosatellite-DXZ4
23	114965558	114967514	1.956	958	670	macrosatellite-DXZ4
23	114968541	114969796	1.255	257	1027	macrosatellite-DXZ4
23	114969798	114970852	1.054	56	2	macrosatellite-DXZ4
23	114971520	114973552	2.032	871	668	macrosatellite-DXZ4
23	114974777	114976822	2.045	1047	1225	macrosatellite-DXZ4
23	114977502	114979813	2.311	1313	680	macrosatellite-DXZ4

23	114980485	114982796	2.311	1313	672	macrosatellite-DXZ4
23	114983470	114985781	2.311	1313	674	macrosatellite-DXZ4
23	114986449	114988760	2.311	1313	668	macrosatellite-DXZ4
23	114989702	114991747	2.045	1047	942	macrosatellite-DXZ4
23	114992405	114994716	2.311	1313	658	macrosatellite-DXZ4
23	114995398	114997709	2.311	1313	682	macrosatellite-DXZ4
23	114998885	115000439	1.554	224	1176	macrosatellite-DXZ4
23	118572124	118573459	1.335	237	3571685	SLC25A43
23	120064672	120066902	2.230	1232	1491213	CT47A-family
23	120069533	120071763	2.230	1232	2631	CT47A-family
23	120074394	120076624	2.230	1232	2631	CT47A-family
23	120079254	120081484	2.230	1232	2630	CT47A-family
23	120084115	120086345	2.230	1232	2631	CT47A-family
23	120088975	120090501	1.526	351	2630	CT47A-family
23	120094352	120096088	1.736	707	3851	CT47A-family
23	120098719	120100949	2.230	1232	2631	CT47A-family
23	120103579	120105809	2.230	1232	2630	CT47A-family
23	120108439	120110669	2.230	1232	2630	CT47A-family
23	120113299	120115529	2.230	1232	2630	CT47A-family
23	120118159	120120389	2.230	1232	2630	CT47A-family